Editors' Suggestion

Coexistence of Insulatorlike Paramagnon and Metallic Spin-Orbit Exciton Modes in $SrIrO_3$

E. Paris,[1,*] W. Zhang,[1] Y. Tseng,[1,2] A. Efimenko,[3] C. Sahle,[3] V. N. Strocov,[1] E. Skoropata,[1] K. Rolfs,[4] T. Shang,[4,5] J. Lyu,[4,6] E. Pomjakushina,[4] M. Medarde,[4] H. M. Rønnow,[7] B. Normand,[8,7] M. Radovic,[1] and T. Schmitt[1,†]

[1]PSI Center for Photon Sciences, CH-5232 Villigen-PSI, Switzerland
[2]Institute of Physics, National Yang Ming Chiao Tung University, Hsinchu 300093, Taiwan
[3]European Synchrotron Radiation Facility, 71 Avenue des Martyrs, 38043 Grenoble, France
[4]PSI Center for Neutron and Muon Sciences, CH-5232 Villigen-PSI, Switzerland
[5]Key Laboratory of Polar Materials and Devices (MOE), School of Physics and Electronic Science, East China Normal University, Shanghai 200241, China
[6]CAS Key Laboratory of Magnetic Materials and Devices, Ningbo Institute of Materials Technology and Engineering, Chinese Academy of Sciences, Ningbo 315201, China
[7]Institute of Physics, Ecole Polytechnique Fédérale de Lausanne (EPFL), CH-1015 Lausanne, Switzerland
[8]PSI Center for Scientific Computing, Theory and Data, CH-5232 Villigen-PSI, Switzerland

(Received 11 December 2024; revised 8 August 2025; accepted 10 October 2025; published 31 October 2025)

We probe the spectrum of elementary excitations in $SrIrO_3$ by using heterostructured $[(SrIrO_3)_m/(SrTiO_3)_l]$ samples to approach the bulk limit. Our resonant inelastic x-ray scattering (RIXS) measurements at the Ir L_3 edge reveal a robust low-lying collective magnetic mode with an antiferromagnetic (AFM) dispersion similar to the insulators Sr_2IrO_4 and $Sr_3Ir_2O_7$, albeit with a large gap and much larger linewidth. At higher energies we find the spin-orbit exciton, also strongly broadened, but with an inverted dispersion and doubled periodicity that are controlled by the charge hopping. These results demonstrate that the AFM paramagnon persists, somewhat counterintuitively, far into the metallic regime of the insulator-metal transition driven by the degree of confinement in the heterostructure. We conclude that these two excitations, which are contrasting but coexisting hallmarks of strong AFM pseudospin and charge fluctuations in a spin-orbit-coupled Mott-Slater material, are properties intrinsic to the ground state of semimetallic perovskite $SrIrO_3$.

DOI: 10.1103/96fl-5zlh

Iridium oxides of the Ruddlesden-Popper series $Sr_{n+1}Ir_nO_{3n+1}$ have attracted extensive interest in the search for unconventional phenomena arising from the interplay between strong electronic correlations and large spin-orbit coupling (SOC) [1–5]. Although the compounds Sr_2IrO_4 and $Sr_3Ir_2O_7$, which exhibit collective charge localization and antiferromagnetic (AFM) ordering of the spin-orbit-entangled $J = 1/2$ pseudospins, have been classified as spin-orbit Mott insulators (MIs), their energy gap is one order of magnitude smaller than that of a typical $3d$ MI. Indeed the end member of the series, $SrIrO_3$, appears to be a nonmagnetic, multiband semimetal [6–8], whose remarkably narrow low-lying electronic bands and significant admixture of $J = 1/2$ and $3/2$ states indicate that these materials lie in the intermediate-coupling, or "Mott-Slater" regime [9,10]. Further, the prediction that SOC makes $SrIrO_3$ a Dirac semimetal [11] places it at an exciting nexus of condensed matter physics where correlated quantum materials with competing spin, charge, and lattice [7] energy scales converge with topological phenomena [12].

Nevertheless, the true properties of perovskite $SrIrO_3$ have remained enigmatic due to the unavailability of single-crystal samples. The SOC-induced coexistence of heavy and light carriers [7,13] mixes the transport and magnetic properties to produce strong magnetoresistance [8,9] and spin-Hall effects [14], which have potential for low-power spintronic applications [15–18]. The observation of non-Fermi-liquid transport characteristics has been interpreted as a hallmark of proximity to a metal-insulator transition (MIT) [2,13,19]. Contrary to expectations based on the $4d$ analog, $SrRuO_3$, the insulating phase proximate to $SrIrO_3$ appears to be AFM, and has been reached by the application of chemical pressure [20,21]. The extreme interest in unraveling the complex electronic and magnetic structure of $SrIrO_3$ has led a number of authors to investigate dimensionality effects using $[(SrIrO_3)_m/(SrTiO_3)_l]$ heterostructures

*Contact author: eugenio.paris@psi.ch
†Contact author: thorsten.schmitt@psi.ch

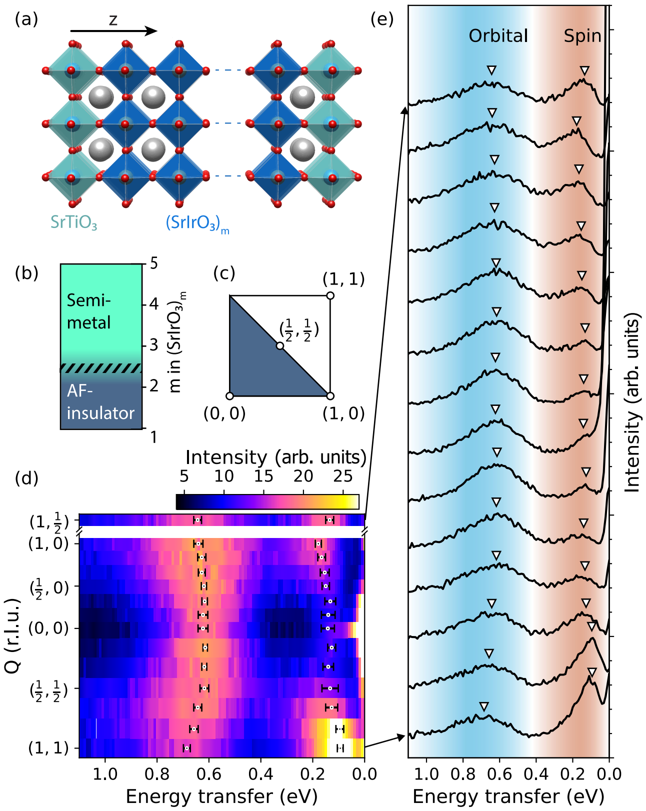

FIG. 1. RIXS investigation of $(SrIrO_3)_m(SrTiO_3)_l$ heterostructures. (a) Representation of $(SrIrO_3)_m(SrTiO_3)_1$ heterostructures, which were grown on a (001)-oriented $SrTiO_3$ single-crystal substrate. The samples investigated here had $m = 3$, 4, and 7 with $l = 1$ and $m = 10$ with $l = 4$. (b) Phase diagram of the $(SrIrO_3)_m(SrTiO_3)_l$ system, illustrating the bandwidth-controlled MIT [24] that takes place as the confinement is increased from $m = 3$ to 2 [22]. (c) Reciprocal space of the pseudocubic AFM unit cell. (d) Compilation of Ir L_3-edge RIXS spectra at all measured $\vec{Q}$ points for the $m = 4$ sample at $T = 20$ K. (e) Intensity data of panel (d) shown as a function of energy transfer for every $\vec{Q}$ point. We identify a low-energy spin excitation (light red) and a spin-orbit exciton at intermediate energies (light blue).

[Fig. 1(a)]. These studies found that the confinement-driven MIT between $m = 2$ and 3 heterostructures [Fig. 1(b)] reproduces the n-driven MIT of bulk $Sr_{n+1}Ir_nO_{3n+1}$ [19,22,23], but left unexplored the spectrum of spin, charge, and orbital excitations on the metallic side.

In this Letter we use resonant inelastic x-ray scattering (RIXS) to analyze the low-lying collective excitations of $SrIrO_3/SrTiO_3$ heterostructures spanning the metallic regime beyond the MIT. In every case from $m = 3$ (significantly confined) to $m = 10$ (the putative bulk analog), we find a dispersive magnetic excitation similar to the pseudospin-wave modes of single-crystalline Sr_2IrO_4 and $Sr_3Ir_2O_7$, except in that it has a large gap and up to double the linewidth. Counterintuitively, we also find in every case that the d-d transitions form a clear, if broad, spin-orbit exciton (SOE) whose dispersion is dominated by metallic charge motion. Both modes are largely insensitive to the degree of confinement, and hence we deduce that strong and short-ranged AFM pseudospin correlations critically damped by metallic charge fluctuations are the intrinsic physics of the multiband, Mott-Slater semimetallic phase of perovskite $SrIrO_3$.

To study the excitations on the metallic side of the confinement-driven MIT, we prepared three high-repetition superlattice heterostructures of the form $[(SrIrO_3)_m(SrTiO_3)] \times 70$, with $m = 3$, 4, and 7, and one of the form $[(SrIrO_3)_{10}(SrTiO_3)_4] \times 8$. All four samples were grown epitaxially on a single-crystal $SrTiO_3$ (001) substrate using pulsed laser deposition and their layer structure is represented schematically in Fig. 1(a). Sample growth and characterization details are presented in Sec. S1 of Supplemental Material [25].

RIXS is a method of choice for probing magnetic fluctuations with 100 meV energy scales in strongly correlated materials [31–35], and is unique in providing momentum-resolved information for thin-film systems. RIXS has been used to investigate the perovskite iridates in their bulk [36–40] and thin-film forms [41,42], and for studies of the two insulating $[(SrIrO_3)_m(SrTiO_3)_1]$ heterostructures, namely, $m = 1$ and 2 [43,44].

Our Ir L_3-edge (11.2145 keV) RIXS experiments were performed at the ID20 beam line [45] of the European Synchrotron Radiation Facility. We varied the momentum transfer to cover the (Q_x, Q_y) plane [Fig. 1(c)], with the z-axis component fixed to $Q_z = 3.67 \pm 0.01$ r.l.u. (indexed to the unit cell of $SrTiO_3$). The sample temperature was set to 20 K.

The RIXS spectra of all four systems exhibited the same overall features, and we use the example of the $m = 4$ heterostructure, shown in Figs. 1(d) and 1(e), to summarize these. All spectra have an intense peak near zero energy whose fit (to elastic scattering processes and a weak phonon contribution) is discussed in Sec. S2 of Supplemental Material [25]. In the energy-loss region 50–300 meV, the spectra exhibit a dispersive excitation with energy minima at the zone center and (1,1) points, and maxima on the boundary of the putative AFM Brillouin zone, whose energy is qualitatively similar to the pseudospin-wave modes reported in Sr_2IrO_4 and $Sr_3Ir_2O_7$[36,37]. In the range 0.5–0.8 eV, the spectra show a further broad and dispersive peak that is common to many Ir oxides and has its origin in d-d orbital excitations [36,46,47].

In Fig. 2 we present a quantitative analysis of the RIXS spectra at three different $\vec{Q}$ values for all four heterostructures in our series, stacked to illustrate their approach to the bulk limit. Definitely our most striking qualitative result is that both the pseudospin wave and the collective orbital mode are so similar in all respects, despite the heterostructures varying from a "minimal metallic" configuration ($m = 3$ has only one "bulk" IrO_2 plane and one pair of interfacial planes) to one that should truly emulate the bulk. Perhaps the next most obvious feature is that the excitations of every heterostructure at every $\vec{Q}$ are extremely broad

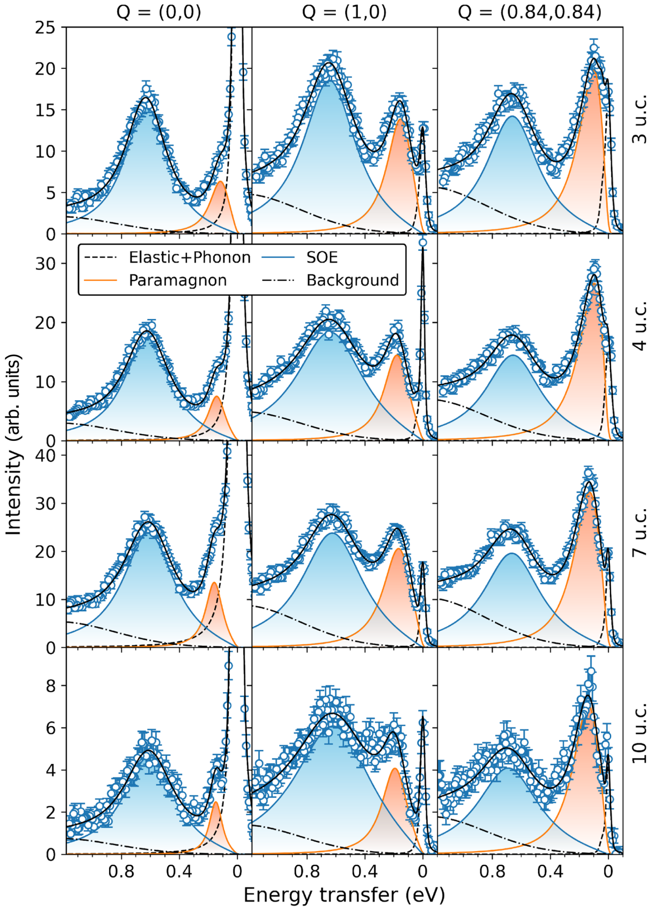

FIG. 2. RIXS spectra. Ir L_3-edge spectra at selected momenta shown for our four samples. Measured intensity data (symbols) presented together with a best fit (black line) composed of elastic and phonon (dashed), paramagnon (light red), spin-orbit exciton (SOE, light blue), and high-energy contributions (dot-dashed), as detailed in Sec. S2 of Supplemental Material [25].

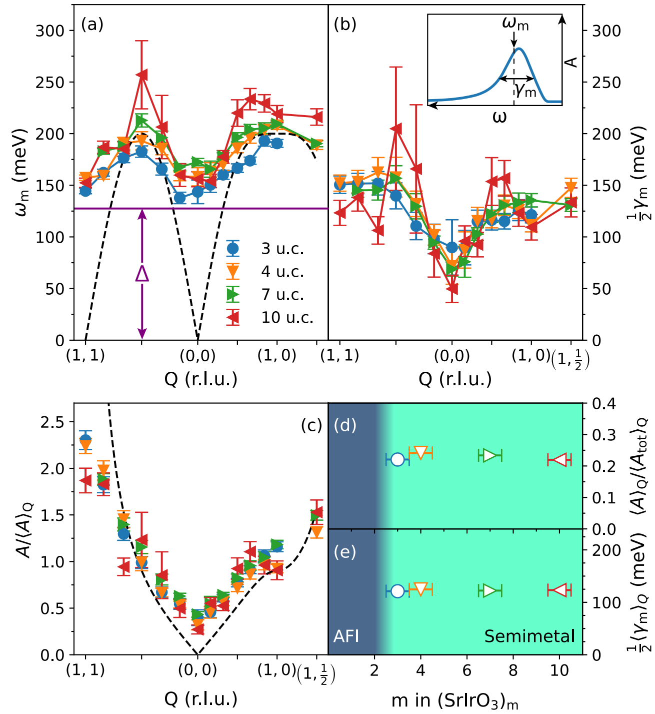

FIG. 3. Paramagnon dispersion, linewidth, and intensity. (a) Momentum dependence of the energy, $\omega_m(\vec{Q})$, of the collective magnetic mode, extracted by fitting to the DHO model, for all four samples. The dashed black line shows the dispersion of the square-lattice Heisenberg AFM for $J = 100$ meV and the solid purple line the finite-size gap, Δ, arising due to the ultrashort correlation length, $\xi/a \approx 1$. (b) Momentum dependence of the corresponding paramagnon linewidths, $\gamma_m(\vec{Q})/2$, and (c) of the paramagnon spectral weights, $A(\vec{Q})$, normalized to the $\vec{Q}$-averaged magnetic weight. The black dashed line in (c) is the result for the square-lattice Heisenberg AFM scaled by an arbitrary constant. (d) $\vec{Q}$-averaged magnetic weight normalized by the total spectral weight and shown as a function of the $SrIrO_3$ layer thickness, m. (e) Paramagnon linewidth, $\gamma_m(\vec{Q})/2$, averaged over $\vec{Q}$ and shown as a function of m.

(Fig. 2), indicating intrinsically ultrashort-range spin and orbital correlations.

In detail, we performed a multicomponent fit of each spectrum to separate the contributions of the near-elastic processes, pseudospin and orbital excitations, and a high-energy contribution (Fig. 2), as described in Sec. S2 of Supplemental Material [25]. We modeled the broad excitations with the damped harmonic oscillator (DHO) profile used to describe the strongly damped paramagnons observed in a number of doped cuprates [48,49] and iron-based superconductors [33,50–52]. The key property of this form [inset Fig. 3(b), and Sec. S2 [25]] is that it can be used equally when the linewidth, $\gamma_i(\vec{Q})/2$, exceeds the bare propagation frequency, $\omega_i(\vec{Q})$, a regime we approach in parts of the Brillouin zone (below). As Fig. 2 makes clear, this functional form provides a good fit to the measured line shapes of both excitations for all samples at all momenta.

In Fig. 3 we show the dispersions, linewidths, and normalized intensities that we extract for the paramagnon in each of our samples. First, the dispersion [Fig. 3(a)] is very similar in all four cases. It has a generic form familiar from that of magnons arising from nearest-neighbor AFM interactions with a maximum around 200 meV along the zone boundary (black dashed line), except with a huge gap, Δ, of over 130 meV at the zone center and a giant damping that is a large fraction of the band energy [Fig. 3(b)]. Second, this dispersion is similar to that reported for the $m = 1$ and 2 heterostructures [43,44], which are thought to be strongly confined and insulating systems. Because the confinement-driven MIT occurs at $2 < m < 3$ [Fig. 1(b)], it is very surprising to find that our samples all exhibit near-identical RIXS spectra despite being paramagnetic semimetals. In particular, the bulk-type transport and magnetic properties of $m = 10$ samples [22,23] attest that these are well in the semimetallic phase. Thus we deduce that this gapped and strongly damped AFM pseudospin wave is not related to confinement effects in a near-ordered insulator, but is rather an intrinsic property of the bulk semimetal.

We interpret the situation as follows. Although the modes of the $m = 1$ and 2 heterostructures have been associated with the spin waves of bulk Sr_2IrO_4 and $Sr_3Ir_2O_7$ [43], the damping is much larger at all momenta and the large gap in all the heterostructures, metallic or insulating, well exceeds the values obtained in either material. In fact the two are quite different, with Sr_2IrO_4 behaving as a true MI and square-lattice Heisenberg AFM, showing a large charge gap and minimal spin gap [53,54], whereas $Sr_3Ir_2O_7$ has an interlayer spin gap [36] and a charge gap [55] of the same order as the magnetic energy scale [38,39], which is a characteristic of the Mott-Slater regime [9,10]. The giant paramagnon linewidth observed in both insulating [43] and metallic heterostructures [Fig. 3(b)], $\gamma_m \approx \omega_m$, is a hallmark of near-unitary scattering, which limits the lifetime $\tau = 1/\gamma_m$, and hence the spin correlation length ($\xi \approx a$), to the nearest-neighbor (n.n.) level, while the opening of the huge gap, $\Delta \approx J(a/\xi)$, in Fig. 3(a) is a finite-size effect stemming from the correspondingly tiny correlated magnetic regions.

To characterize this strong scattering, we first note that the $\vec{Q}$ dependence of the peak intensity is also nearly identical for all four samples [Fig. 3(c)], with its maximum at $\vec{Q} = (1, 1)$ and minimum at $\vec{Q} = (0, 0)$ again characteristic of a square-lattice Heisenberg AFM [56]. Next we observe that the dispersions in Fig. 3(a) show only minor bandwidth changes, falling from around 80 meV in the bulk limit ($m = 10$) to 60 meV in our more confined samples. The slight increase in the zone-boundary energy as the electronic system is deconfined suggests the role of interactions with the charge carriers.

Before pursuing this, we finish our discussion of the paramagnon linewidth shown in Fig. 3(b). This varies by a factor of 2 from the zone center to the zone edge, but its $\vec{Q}$ average changes remarkably little with the degree of confinement across the heterostructure series, as we show in Fig. 3(e). While hybridization with the TiO_2 layers and effective doping of the interfacial IrO_2 layers cannot be excluded as factors contributing to the strong damping, at minimum our $m = 10$ sample has rather few interfacial layers and thus one expects that the right-hand side of Fig. 3(e) provides a good estimate of the intrinsic damping in bulk $SrIrO_3$. As a further probe of possible interfacial effects, in Fig. 3(d) we show the average magnetic intensity normalized to the total spectral intensity, and again find no meaningful change. This result constitutes one of our most important indicators that all the features we observe are intrinsic to the $SrIrO_3$ system, as distinct modes of the interfacial IrO_2 layers would be expected to scale as $1/m$.

Turning now to the orbital excitation, we apply the same DHO analysis to extract the energy and linewidth. Figure 4(a) shows that this excitation forms a broad and dispersive mode with a bandwidth of 100 meV, conventionally described as a “spin-orbit exciton” (SOE) [36,47,57–59]. In Fig. 4(a) it is difficult to discern much change in its dispersion caused by the confinement. As one might anticipate from Fig. 2, the linewidth of the SOE is very high, and Fig. 4(b) shows that, like the damping of the paramagnon [Fig. 3(b)] it also varies by 80–120 meV as a function of $\vec{Q}$. In this case we note a systematic trend towards a larger linewidth as the confinement is removed, quantified in Fig. 4(c), which contrasts with the behavior of the paramagnon and presumably reflects the progressive delocalization of electrons contributing to the relevant scattering processes.

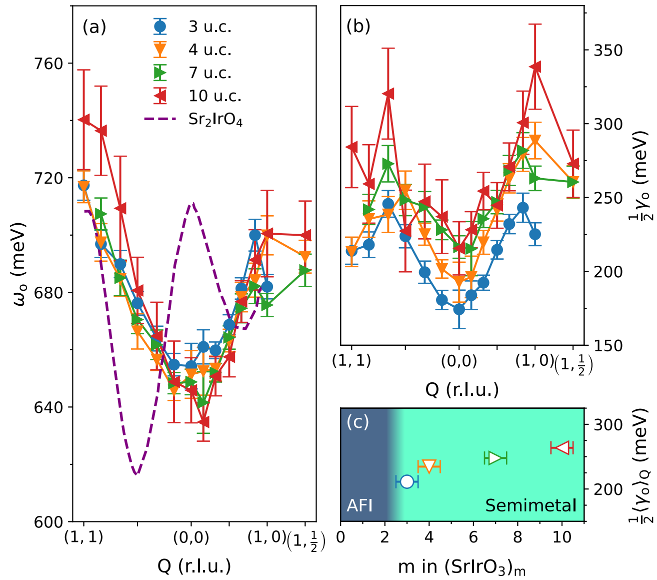

FIG. 4. Spin-orbital exciton. (a) Momentum dependence of the SOE excitation energy, $\omega_o(\vec{Q})$, extracted from the DHO fit for all four samples. The purple line shows the SOE dispersion in Sr_2IrO_4, taken from the data of Ref. [36] as described in Sec. S3 of Supplemental Material [25]. (b) Momentum dependence of the corresponding linewidth, $\gamma_o(\vec{Q})/2$. (c) $\gamma_o(\vec{Q})/2$ averaged over $\vec{Q}$ and shown as a function of m.

Returning to Fig. 4(a), the dispersion of the SOE is completely different from that of Sr_2IrO_4 [36,47], whose form is characteristic of a magnetic insulator. Instead, the upward dispersion around $\vec{Q} = (0, 0)$ follows the form found in the paramagnetic metal Sr_2RhO_4 [58] and the doubled $\vec{Q}$-space periodicity relative to Sr_2IrO_4 [purple line in Fig. 4(a)] shows no evidence of AFM character. From this result we conclude that, despite the short-range-correlated magnetic background in $SrIrO_3$ systems, the propagation of the SOE is dominated by metallic hopping processes of the conduction electrons.

The origin of such strongly contrasting SOE behavior is that the physics of the AFM insulator is governed by the narrow, filled lower Hubbard-type band formed from the $J = 1/2$ electronic states, whereas in a metallic system it is controlled by charge hopping in the $J = 3/2$ band [58].

The surprise in our results is that a paramagnon so similar to the AFM insulator coexists with a manifestly metallic SOE. A clue to this coexistence is provided by the behavior of both hole- [40] and electron-doped [60] Sr_2IrO_4, where the paramagnon and the constraining effect of the magnetic background on the mobile holes persists out to dopings in excess of 10%. Thus the paramagnon can retain its definition also when "self-doping" of the upper $J = 1/2$ band occurs as the $J = 3/2$ band becomes broad enough to make the system metallic. The finite concentration of carriers causing the bad-metal transport characteristics, whose correlation-controlled charge fluctuations cause the giant linewidths, also decouples the behavior of the SOE from the physics of the narrow $J = 1/2$ band. The fact that the SOEs of both heterostructured and bulk $SrIrO_3$ systems can be so different from Sr_2IrO_4, while the magnetic dispersion has so many similarities, underlines the complex interplay of structure and correlations in this class of materials [61].

A further important argument that the giant paramagnon damping is an intrinsic property of $SrIrO_3$ can be found in the extensive reports of non-Fermi-liquid and quantum critical behavior in this material [2,13,62]. $SrIrO_3$ heterostructures exhibit the fingerprints of both Mott physics, in the form of the bad-metal (or strange-metal) resistivities [22], and Slater physics, in the form of the strong AFM spin fluctuations we observe despite the charge being delocalized. Indeed the emerging theoretical consensus [9,10] places $SrIrO_3$ in the Mott-Slater regime of intermediate correlations. Our observation of near-critically damped magnetic and orbital fluctuations ($\gamma_i \approx \omega_i$) indicates that their mean free path is of order one lattice constant ($\xi/a \approx 1$), which stands to reason if the Mott-Slater charge fluctuations drive the system towards the Mott-Ioffe-Regel limit. This very-bad-metal behavior of the quasiparticle scattering in $SrIrO_3$ has also been shown [13] to approach the Planckian limit [63] at finite temperatures.

Finally, the most important issue when drawing our conclusions from heterostructures concerns the effect of the TiO_2 layers. It is known that Ti-O-Ir hybridization occurs [22,64], that the AFM ground state at $m = 1$ changes with the $SrTiO_3$ thickness ($l > 1$) [65], and that the $m = 1$ magnon dispersion changes slightly when using $CaTiO_3$ [44]. The rotation and distortion of IrO_6 octahedra caused by the lattice mismatch are also found to affect the interfacial layers [7,43,66]. To judge whether the properties we observe could be a consequence of heterostructuring, rather than being intrinsic to $SrIrO_3$, we have argued that they should show a systematic dependence on the layer thickness. This was not the case for the paramagnon broadening in Fig. 3(e) or the SOE broadening in Fig. 4(c). More specifically, if a mode were interfacial, its spectral weight should be proportional to the interface or bulk ratio of the different samples. As we showed in Fig. 3(d), the intensity of the paramagnon is a rather steady 22%–24% of the total weight, even as the nominal ratio of interfacial IrO_2 layers changes from 67% to 20%. To complete this argument, we probed the local chemical environment of the interfaces by Ti L-edge x-ray absorption spectroscopy (XAS), as we detail in Sec. S1B of Supplemental Material [25]. This confirmed first that finite Ti-O-Ir hybridization takes place and second that the XAS intensities from Ti atoms in different environments do scale linearly with the nominal ratio given by the heterostructure geometry. Hence the magnetic mode we observe must be a property of the bulk, while the hybridization remains a minor quantitative effect.

In summary, we have performed RIXS measurements to unveil the spectrum of elementary excitations in heterostructured $SrIrO_3$. Investigating a series of systems on the semimetallic side of the confinement-driven MIT confirms the presence in all spectra of two universal features that are also shared with the AFM insulator. At low energy is a broad and gapped pseudospin paramagnon that reveals the simultaneous presence of strong AFM correlations and strong quasiparticle scattering. In counterpoint is a spin-orbit exciton at higher energy, whose dispersion and extreme linewidth reflect only the rapid charge fluctuations of semimetallic $SrIrO_3$, and not the strong AFM character. However, charge fluctuations arising from the non-Fermi-liquid nature of the strange-metal phase in $SrIrO_3$ cause the magnetic fluctuations to remain ultrashort-ranged, and hence provide additional evidence for a quasiparticle scattering rate near the unitary limit. The remarkable robustness of both nominally incompatible excitations, the AFM paramagnon as confinement is removed and the metallic spin-orbit exciton as confinement is increased, leads us to conclude that both are generic properties of bulk $SrIrO_3$.

Acknowledgments—We thank V. Favre and X. Lu for helpful contributions. This work was supported by the Swiss National Science Foundation through the Sinergia network Mott Physics Beyond the Heisenberg Model (MPBH, Research Grants No. CRSII2 160765/1 and No. CRSII2 141962) and through research Project No. 200021 178867. We acknowledge the ESRF for the provision of beam-time on ID20 under Proposal No. STD-HC-3997. The Ti L-edge XAS was performed at the ADRESS beam line of the Swiss Light Source at the Paul Scherrer Institut (PSI).

Data availability—The data that support the findings of this article are openly available [67], embargo periods may apply.

[1] B. J. Kim, H. Jin, S. J. Moon, J. Y. Kim, B. G. Park, C. S. Leem, J. Yu, T. W. Noh, C. Kim, S. J. Oh, J. H. Park, V. Durairaj, G. Cao, and E. Rotenberg, Novel $j_{\mathrm{eff}} = 1/2$ Mott state induced by relativistic spin-orbit coupling in Sr_2IrO_4, Phys. Rev. Lett. **101**, 076402 (2008).

[2] S. J. Moon, H. Jin, K. W. Kim, W. S. Choi, Y. S. Lee, J. Yu, G. Cao, A. Sumi, H. Funakubo, C. Bernhard, and T. W. Noh, Dimensionality-controlled insulator-metal transition and correlated metallic state in 5d transition metal oxides $Sr_{n+1}Ir_nO_{3n+1}$ ($n = 1$, 2, and ∞), Phys. Rev. Lett. **101**, 226402 (2008).

[3] H. Watanabe, T. Shirakawa, and S. Yunoki, Microscopic study of a spin-orbit-induced Mott insulator in Ir oxides, Phys. Rev. Lett. **105**, 216410 (2010).

[4] C. Martins, M. Aichhorn, L. Vaugier, and S. Biermann, Reduced effective spin-orbital degeneracy and spin-orbital ordering in paramagnetic transition-metal oxides: Sr_2IrO_4 versus Sr_2RhO_4, Phys. Rev. Lett. **107**, 266404 (2011).

[5] R. Arita, J. Kuneš, A. V. Kozhevnikov, A. G. Eguiluz, and M. Imada, *Ab initio* studies on the interplay between spin-orbit interaction and Coulomb correlation in Sr_2IrO_4 and Ba_2IrO_4, Phys. Rev. Lett. **108**, 086403 (2012).

[6] Z. T. Liu, M. Y. Li, Q. F. Li, J. S. Liu, W. Li, H. F. Yang, Q. Yao, C. C. Fan, X. G. Wan, Z. Wang, and D. W. Shen, Direct observation of the Dirac nodes lifting in semimetallic perovskite $SrIrO_3$ thin films, Sci. Rep. **6**, 30309 (2016).

[7] Y. F. Nie, P. D. C. King, C. H. Kim, M. Uchida, H. I. Wei, B. D. Faeth, J. P. Ruf, J. P. C. Ruff, L. Xie, X. Pan, C. J. Fennie, D. G. Schlom, and K. M. Shen, Interplay of spin-orbit interactions, dimensionality, and octahedral rotations in semimetallic $SrIrO_3$, Phys. Rev. Lett. **114**, 016401 (2015).

[8] J. Fujioka, T. Okawa, A. Yamamoto, and Y. Tokura, Correlated Dirac semimetallic state with unusual positive magnetoresistance in strain-free perovskite $SrIrO_3$, Phys. Rev. B **95**, 121102 (2017).

[9] L. Hao, Z. Wang, J. Yang, D. Meyers, J. Sanchez, G. Fabbris, Y. Choi, J.-W. Kim, D. Haskel, P. J. Ryan, K. Barros, J.-H. Chu, M. P. M. Dean, C. D. Batista, and J. Liu, Anomalous magnetoresistance due to longitudinal spin fluctuations in a $J_{\mathrm{eff}} = 1/2$ Mott semiconductor, Nat. Commun. **10**, 5301 (2019).

[10] J. Yang, L. Hao, D. Meyers, T. Dasa, L. Xu, L. Horak, P. Shafer, E. Arenholz, G. Fabbris, Y. Choi, D. Haskel, J. Karapetrova, J.-W. Kim, P. J. Ryan, H. Xu, C. D. Batista, M. P. M. Dean, and J. Liu, Strain-modulated Slater-Mott crossover of pseudospin-half square-lattice in $(SrIrO_3)_1/(SrTiO_3)_1$ superlattices, Phys. Rev. Lett. **124**, 177601 (2020).

[11] M. A. Zeb and H.-Y. Kee, Interplay between spin-orbit coupling and Hubbard interaction in $SrIrO_3$ and related $Pbnm$ perovskite oxides, Phys. Rev. B **86**, 085149 (2012).

[12] Y. Chen, Y.-M. Lu, and H.-Y. Kee, Topological crystalline metal in orthorhombic perovskite iridates, Nat. Commun. **6**, 6593 (2015).

[13] K. Sen, D. Fuchs, R. Heid, K. Kleindienst, K. Wolff, J. Schmalian, and M. Le Tacon, Strange semimetal dynamics in $SrIrO_3$, Nat. Commun. **11**, 4270 (2020).

[14] A. S. Patri, K. Hwang, H.-W. Lee, and Y. B. Kim, Theory of large intrinsic spin Hall effect in iridate semimetals, Sci. Rep. **8**, 8052 (2018).

[15] A. S. Everhardt, M. DC, X. Huang, S. Sayed, T. A. Gosavi, Y. Tang, C.-C. Lin, S. Manipatruni, I. A. Young, S. Datta, J.-P. Wang, and R. Ramesh, Tunable charge to spin conversion in strontium iridate thin films, Phys. Rev. Mater. **3**, 051201 (2019).

[16] T. Nan, T. J. Anderson, J. Gibbons, K. Hwang, N. Campbell, H. Zhou, Y. Q. Dong, G. Y. Kim, D. F. Shao, T. R. Paudel, N. Reynolds, X. J. Wang, N. X. Sun, E. Y. Tsymbal, S. Y. Choi, M. S. Rzchowski, Y. B. Kim, D. C. Ralph, and C. B. Eom, Anisotropic spin-orbit torque generation in epitaxial $SrIrO_3$ by symmetry design, Proc. Natl. Acad. Sci. U.S.A. **116**, 16186 (2019).

[17] L. Liu, Q. Qin, W. Lin, C. Li, Q. Xie, S. He, X. Shu, C. Zhou, Z. Lim, J. Yu, W. Lu, M. Li, X. Yan, S. J. Pennycook, and J. Chen, Current-induced magnetization switching in all-oxide heterostructures, Nat. Nanotechnol. **14**, 939 (2019).

[18] J. Yang, H. Zhang, H. Zhang, and L. Hao, Perspective on antiferromagnetic iridates for spintronics, APL Mater. **11**, 070901 (2023).

[19] D. J. Groenendijk, C. Autieri, J. Girovsky, M. C. Martinez-Velarte, N. Manca, G. Mattoni, A. M. R. V. L. Monteiro, N. Gauquelin, J. Verbeeck, A. F. Otte, M. Gabay, S. Picozzi, and A. D. Caviglia, Spin-orbit semimetal $SrIrO_3$ in the two-dimensional limit, Phys. Rev. Lett. **119**, 256403 (2017).

[20] H. Zheng, J. Terzic, F. Ye, X. G. Wan, D. Wang, J. Wang, X. Wang, P. Schlottmann, S. J. Yuan, and G. Cao, Simultaneous metal-insulator and antiferromagnetic transitions in orthorhombic perovskite iridate $Sr_{0.94}Ir_{0.78}O_{2.68}$ single crystals, Phys. Rev. B **93**, 235157 (2016).

[21] Q. Cui, J.-G. Cheng, W. Fan, A. E. Taylor, S. Calder, M. A. McGuire, J.-Q. Yan, D. Meyers, X. Li, Y. Q. Cai, Y. Y. Jiao, Y. Choi, D. Haskel, H. Gotou, Y. Uwatoko, J. Chakhalian, A. D. Christianson, S. Yunoki, J. B. Goodenough, and J.-S. Zhou, Slater insulator in iridate perovskites with strong spin-orbit coupling, Phys. Rev. Lett. **117**, 176603 (2016).

[22] J. Matsuno, K. Ihara, S. Yamamura, H. Wadati, K. Ishii, V. V. Shankar, H.-Y. Kee, and H. Takagi, Engineering a spin-orbital magnetic insulator by tailoring superlattices, Phys. Rev. Lett. **114**, 247209 (2015).

[23] P. Schütz, D. Di Sante, L. Dudy, J. Gabel, M. Stübinger, M. Kamp, Y. Huang, M. Capone, M.-A. Husanu, V. N. Strocov, G. Sangiovanni, M. Sing, and R. Claessen, Dimensionality-driven metal-insulator transition in spin-orbit-coupled $SrIrO_3$, Phys. Rev. Lett. **119**, 256404 (2017).

[24] S. Kong, L. Li, Z. Lu, J. Feng, X. Zhang, P. Song, Y. Shi, Y. Wang, B. Ge, K. Rolfs, E. Pomjakushina, T. Schmitt, N. C. Plumb, M. Shi, Z. Zhong, M. Radovic, Z. Wang, and R.-W. Li, Isostructural metal-insulator transition driven by dimensional-crossover in $SrIrO_3$ heterostructures, Phys. Rev. Mater. **6**, 034404 (2022).

[25] See Supplemental Material at http://link.aps.org/supplemental/10.1103/96fl-5zlh which include Refs. [26–30], for a detailed discussion of our sample growth and characterization, the RIXS fitting methodology leading to our paramagnon and SOE spectra, and the extraction of the SOE disperson for Sr_2IrO_4 shown in Fig. 4(a).

[26] C. C. Fan, Z. T. Liu, S. H. Cai, Z. Wang, P. Xiang, K. L. Zhang, W. L. Liu, J. S. Liu, P. Wang, Y. Zheng, D. W. Shen, and L. X. You, Reactive molecular beam epitaxial growth and *in situ* photoemission spectroscopy study of iridate superlattices, AIP Adv. **7**, 085307 (2017).

[27] K. R. Kleindienst, K. Wolff, J. Schubert, R. Schneider, and D. Fuchs, Structural properties and anisotropic electronic transport in $SrIrO_3$ films, Phys. Rev. B **98**, 115113 (2018).

[28] V. N. Strocov, T. Schmitt, U. Flechsig, T. Schmidt, A. Imhof, Q. Chen, J. Raabe, R. Betemps, D. Zimoch, J. Krempasky, X. Wang, M. Grioni, A. Piazzalunga, and L. Patthey, High-resolution soft X-ray beamline ADRESS at the Swiss light source for resonant inelastic x-ray scattering and angle-resolved photoelectron spectroscopies, J. Synchrotron Radiat. **17**, 631 (2010).

[29] J. R. L. Mardegan, D. V. Christensen, Y. Z. Chen, S. Parchenko, S. R. V. Avula, N. Ortiz-Hernandez, M. Decker, C. Piamonteze, N. Pryds, and U. Staub, Magnetic and electronic properties at the γ-Al_2O_3/$SrTiO_3$ interface, Phys. Rev. B **99**, 134423 (2019).

[30] M. Moretti Sala, K. Ohgushi, A. Al-Zein, Y. Hirata, G. Monaco, and M. Krisch, $CaIrO_3$: A spin-orbit Mott insulator beyond the $j_{\mathrm{eff}} = 1/2$ ground state, Phys. Rev. Lett. **112**, 176402 (2014).

[31] M. Le Tacon *et al.*, Intense paramagnon excitations in a large family of high-temperature superconductors, Nat. Phys. **7**, 725 (2011).

[32] M. Le Tacon, M. Minola, D. C. Peets, M. Moretti Sala, S. Blanco-Canosa, V. Hinkov, R. Liang, D. A. Bonn, W. N. Hardy, C. T. Lin, T. Schmitt, L. Braicovich, G. Ghiringhelli, and B. Keimer, Dispersive spin excitations in highly overdoped cuprates revealed by resonant inelastic x-ray scattering, Phys. Rev. B **88**, 020501 (2013).

[33] J. Pelliciari, Y. Huang, T. Das, M. Dantz, V. Bisogni, P. O. Velasco, V. N. Strocov, L. Xing, X. Wang, C. Jin, and T. Schmitt, Intralayer doping effects on the high-energy magnetic correlations in NaFeAs, Phys. Rev. B **93**, 134515 (2016).

[34] L. Das *et al.*, Spin-orbital excitations in Ca_2RuO_4 revealed by resonant inelastic x-ray scattering, Phys. Rev. X **8**, 011048 (2018).

[35] H. Lu, M. Rossi, A. Nag, M. Osada, D. F. Li, K. Lee, B. Y. Wang, M. Garcia-Fernandez, S. Agrestini, Z. X. Shen, E. M. Been, B. Moritz, T. P. Devereaux, J. Zaanen, H. Y. Hwang, K.-J. Zhou, and W. S. Lee, Magnetic excitations in infinite-layer nickelates, Science **373**, 213 (2021).

[36] J. Kim, D. Casa, M. H. Upton, T. Gog, Y.-J. Kim, J. F. Mitchell, M. van Veenendaal, M. Daghofer, J. van den Brink, G. Khaliullin, and B. J. Kim, Magnetic excitation spectra of Sr_2IrO_4 probed by resonant inelastic x-ray scattering: Establishing links to cuprate superconductors, Phys. Rev. Lett. **108**, 177003 (2012).

[37] J. Kim, A. H. Said, D. Casa, M. H. Upton, T. Gog, M. Daghofer, G. Jackeli, J. Van Den Brink, G. Khaliullin, and B. J. Kim, Large spin-wave energy gap in the bilayer iridate $Sr_3Ir_2O_7$: Evidence for enhanced dipolar interactions near the Mott metal-insulator transition, Phys. Rev. Lett. **109**, 157402 (2012).

[38] M. Moretti Sala, V. Schnells, S. Boseggia, L. Simonelli, A. Al-Zein, J. G. Vale, L. Paolasini, E. C. Hunter, R. S. Perry, D. Prabhakaran, A. T. Boothroyd, M. Krisch, G. Monaco, H. M. Rønnow, D. F. McMorrow, and F. Mila, Evidence of quantum dimer excitations in $Sr_3Ir_2O_7$, Phys. Rev. B **92**, 024405 (2015).

[39] X. Lu, D. E. McNally, M. Moretti Sala, J. Terzic, M. H. Upton, D. Casa, G. Ingold, G. Cao, and T. Schmitt, Doping evolution of magnetic order and magnetic excitations in $(Sr_{1-x}La_x)_3Ir_2O_7$, Phys. Rev. Lett. **118**, 027202 (2017).

[40] J. P. Clancy, H. Gretarsson, M. H. Upton, J. Kim, G. Cao, and Y.-J. Kim, Magnetic excitations in hole-doped Sr_2IrO_4: Comparison with electron-doped cuprates, Phys. Rev. B **100**, 104414 (2019).

[41] A. Lupascu, J. P. Clancy, H. Gretarsson, Z. Nie, J. Nichols, J. Terzic, G. Cao, S. S. A. Seo, Z. Islam, M. H. Upton, J. Kim, D. Casa, T. Gog, A. H. Said, V. M. Katukuri, H. Stoll, L. Hozoi, J. van den Brink, and Y.-J. Kim, Tuning magnetic coupling in Sr_2IrO_4 thin films with epitaxial strain, Phys. Rev. Lett. **112**, 147201 (2014).

[42] E. Paris, Y. Tseng, E. M. Pärschke, W. Zhang, M. H. Upton, A. Efimenko, K. Rolfs, D. E. McNally, L. Maurel, M. Naamneh, M. Caputo, V. N. Strocov, Z. Wang, D. Casa, C. W. Schneider, E. Pomjakushina, K. Wohlfeld, M. Radovic, and T. Schmitt, Strain engineering of the charge and spin-orbital interactions in Sr_2IrO_4, Proc. Natl. Acad. Sci. U.S.A. **117**, 24764 (2020).

[43] D. Meyers *et al.*, Magnetism in iridate heterostructures leveraged by structural distortions, Sci. Rep. **9**, 4263 (2019).

[44] J. Yang, H. Suwa, D. Meyers, H. Zhang, L. Horak, Z. Wang, G. Fabbris, Y. Choi, J. Karapetrova, J.-W. Kim, D. Haskel, P. J. Ryan, M. Dean, L. Hao, and J. Liu, Quasi-two-dimensional anomalous Hall Mott insulator of topologically engineered $J_{\mathrm{eff}} = 1/2$ Electrons, Phys. Rev. X **12**, 031015 (2022).

[45] M. Moretti Sala, C. Henriquet, L. Simonelli, R. Verbeni, and G. Monaco, High energy-resolution set-up for Ir L_3-edge RIXS experiments, J. Electron Spectrosc. Relat. Phenom. **188**, 150 (2013).

[46] H. Gretarsson, J. P. Clancy, X. Liu, J. P. Hill, E. Bozin, Y. Singh, S. Manni, P. Gegenwart, J. Kim, A. H. Said, D. Casa, T. Gog, M. H. Upton, H. S. Kim, J. Yu, V. M. Katukuri, L. Hozoi, J. Van Den Brink, and Y. J. Kim, Crystal-field splitting and correlation effect on the electronic structure of A_2IrO_3, Phys. Rev. Lett. **110**, 076402 (2013).

[47] J. Kim, M. Daghofer, A. H. Said, T. Gog, J. van den Brink, G. Khaliullin, and B. J. Kim, Excitonic quasiparticles in a spin-orbit Mott insulator, Nat. Commun. **5**, 4453 (2014).

[48] J. Lamsal and W. Montfrooij, Extracting paramagnon excitations from resonant inelastic x-ray scattering experiments, Phys. Rev. B **93**, 214513 (2016).

[49] H. C. Robarts, M. Barthélemy, K. Kummer, M. Garcia-Fernandez, J. Li, A. Nag, A. C. Walters, K. J. Zhou, and S. M. Hayden, Anisotropic damping and wave vector dependent susceptibility of the spin fluctuations in $La_{2-x}Sr_xCuO_4$ studied by resonant inelastic x-ray scattering, Phys. Rev. B **100**, 214510 (2019).

[50] M. C. Rahn, K. Kummer, N. B. Brookes, A. A. Haghighirad, K. Gilmore, and A. T. Boothroyd, Paramagnon dispersion in β-FeSe observed by Fe L-edge resonant inelastic x-ray scattering, Phys. Rev. B **99**, 014505 (2019).

[51] F. A. Garcia, O. Ivashko, D. E. McNally, L. Das, M. M. Piva, C. Adriano, P. G. Pagliuso, J. Chang, T. Schmitt, and C. Monney, Anisotropic magnetic excitations and incipient Néel order in $Ba(Fe_{1-x}Mn_x)_2As_2$, Phys. Rev. B **99**, 115118 (2019).

[52] X. Lu, W. Zhang, Y. Tseng, R. Liu, Z. Tao, E. Paris, P. Liu, T. Chen, V. N. Strocov, Y. Song, R. Yu, Q. Si, P. Dai,

and T. Schmitt, Spin-excitation anisotropy in the nematic state of detwinned FeSe, Nat. Phys. **18**, 806 (2022).

[53] S. Calder, D. M. Pajerowski, M. B. Stone, and A. F. May, Spin-gap and two-dimensional magnetic excitations in Sr_2IrO_4, Phys. Rev. B **98**, 220402(R) (2018).

[54] J. Bertinshaw, J. K. Kim, J. Porras, K. Ueda, N. H. Sung, A. Efimenko, A. Bombardi, J. Kim, B. Keimer, and B. J. Kim, Spin-wave gap collapse in Rh-doped Sr_2IrO_4, Phys. Rev. B **101**, 094428 (2020).

[55] D. G. Mazzone, Y. Shen, H. Suwa, G. Fabbris, J. Yang, S.-S. Zhang, H. Miao, J. Sears, K. Jia, Y. G. Shi, M. H. Upton, D. M. Casa, X. Liu, J. Liu, C. D. Batista, and M. P. M. Dean, Antiferromagnetic excitonic insulator state in $Sr_3Ir_2O_7$, Nat. Commun. **13**, 913 (2022).

[56] R. Coldea, S. M. Hayden, G. Aeppli, T. G. Perring, D. D. Frost, T. E. Mason, S.-W. Cheong, and Z. Fisk, Spin Waves and Electronic Interactions in La_2CuO_4, Phys. Rev. Lett. **86**, 5377 (2001).

[57] H. Gretarsson, H. Suzuki, H. Kim, K. Ueda, M. Krautloher, B. J. Kim, H. Yavaş, G. Khaliullin, and B. Keimer, Observation of spin-orbit excitations and Hund's multiplets in Ca_2RuO_4, Phys. Rev. B **100**, 045123 (2019).

[58] V. Zimmermann, A. K. Yogi, D. Wong, C. Schulz, M. Bartkowiak, K. Habicht, L. Wang, M. Isobe, M. Minola, G. Khaliullin, B. Keimer, and M. Hepting, Coherent propagation of spin-orbit excitons in a correlated metal, npj Quantum Mater. **8**, 53 (2023).

[59] L. Wang, H. Liu, V. Zimmermann, A. K. Yogi, M. Isobe, M. Minola, M. Hepting, G. Khaliullin, and B. Keimer, Spin-orbit excitons in a correlated metal: Raman scattering study of Sr_2RhO_4, Phys. Rev. Lett. **132**, 116502 (2024).

[60] H. Gretarsson, N. H. Sung, J. Porras, J. Bertinshaw, C. Dietl, J. A. N. Bruin, A. F. Bangura, Y. K. Kim, R. Dinnebier, J. Kim, A. Al-Zein, M. Moretti Sala, M. Krisch, M. Le Tacon, B. Keimer, and B. J. Kim, Persistent paramagnons deep in the metallic phase of $Sr_{2-x}La_xIrO_4$, Phys. Rev. Lett. **117**, 107001 (2016).

[61] P. Liu and C. Franchini, Advanced first-principle modeling of relativistic Ruddlesden-Popper strontium iridates, Appl. Sci. **11**, 2527 (2021).

[62] G. Cao, V. Durairaj, S. Chikara, L. E. DeLong, S. Parkin, and P. Schlottmann, Non-Fermi-liquid behavior in nearly ferromagnetic $SrIrO_3$ single crystals, Phys. Rev. B **76**, 100402 (2007).

[63] G. Grissonanche, Y. Fang, A. Legros, S. Verret, F. Laliberté, C. Collignon, J. Zhou, D. Graf, P. Goddard, L. Taillefer, and B. J. Ramshaw, Linear-in temperature resistivity from an isotropic Planckian scattering rate, Nature (London) **595**, 667 (2021).

[64] S. Y. Kim, C. H. Kim, L. J. Sandilands, C. H. Sohn, J. Matsuno, H. Takagi, K. W. Kim, Y. S. Lee, S. J. Moon, and T. W. Noh, Manipulation of electronic structure via alteration of local orbital environment in $[(SrIrO_3)_m, (SrTiO_3)]$ ($m = 1$, 2, and ∞) superlattices, Phys. Rev. B **94**, 245113 (2016).

[65] L. Hao, D. Meyers, C. Frederick, G. Fabbris, J. Yang, N. Traynor, L. Horak, D. Kriegner, Y. Choi, J.-W. Kim, D. Haskel, P. J. Ryan, M. P. M. Dean, and J. Liu, Two-dimensional $J_{\mathrm{eff}} = 1/2$ antiferromagnetic insulator unraveled from interlayer exchange coupling in artificial perovskite iridate superlattices, Phys. Rev. Lett. **119**, 027204 (2017).

[66] D. Yi, C. L. Flint, P. P. Balakrishnan, K. Mahalingam, B. Urwin, A. Vailionis, A. T. N'Diaye, P. Shafer, E. Arenholz, Y. Choi, K. H. Stone, J.-H. Chu, B. M. Howe, J. Liu, I. R. Fisher, and Y. Suzuki, Tuning perpendicular magnetic anisotropy by oxygen octahedral rotations in $(La_{1-x}Sr_xMnO_3)/(SrIrO_3)$ superlattices, Phys. Rev. Lett. **119**, 077201 (2017).

[67] E. Paris, Data repository for "Coexistence of insulatorlike paramagnon and metallic spin-orbit exciton modes in $SrIrO_3$", Zenodo, 10.5281/zenodo.17350017 (2025).